Bioorganic & Medicinal Chemistry 17 (2009) 8197–8205

Contents lists available at ScienceDirect

Bioorganic & Medicinal Chemistry

journal homepage: www.elsevier.com/locate/bmc

Spectroscopic and biological studies of a novel synthetic chlorin derivative with prospects for use in PDT

Agnieszka Szurko [a,b,*], Marzena Rams [a], Aleksander Sochanik [b], Karolina Sieroń-Stołtny [c], Agnieszka Maria Kozielec [d], Franz-Peter Montforts [d], Roman Wrzalik [a], Alicja Ratuszna [a]

[a] A. Chelkowski Institute of Physics, University of Silesia, Uniwersytecka 4, 40-007 Katowice, Poland
[b] Maria Sklodowska-Curie Memorial Cancer Center and Institute of Oncology, 44-101 Gliwice, Poland
[c] Center for Laser Diagnostics and Therapy, Department and Chair of Internal Diseases, Angiology and Physical Medicine, 41-902 Bytom, Poland
[d] Institute of Organic Chemistry, University of Bremen, D-28359 Bremen, Germany

ARTICLE INFO

Article history:
Received 22 June 2009
Revised 10 October 2009
Accepted 15 October 2009
Available online 20 October 2009

Keywords:
Photodynamic therapy
PDT
Photosensitizers
Synthetic chlorins

ABSTRACT

Photosensitizers with desirable combinations of chemical, photophysical and biological properties are essential for improving the efficacy of photodynamic therapy (PDT) against various cancers. Chlorins seem to be promising candidates for photodynamic therapy (PDT) owing to their photophysical properties. This paper reports spectroscopic and biological properties of a novel synthetic chlorin derivative. Cytotoxicity, phototoxicity as well as subcellular localization of the novel derivative was studied using Lewis lung carcinoma cultured cells (LLC). In the examined concentration range no significant cytotoxic effects were found but high phototoxicity was observed. Confocal laser scanning microscopy demonstrated that the compound, upon entering cells, was localized in the perinuclear cytoplasm of LLC cells. Using fluorescent microscopy we investigated the impact of PDT based on the novel compound upon cytoskeleton and DNA structure of LLC cells. Our results indicate that liposomes are effective in transferring the chlorin photosensitizer into the studied cells, leading to their high photosensitization, whereas the non-carrier delivery mode (i.e., DMSO) is rather useless for such purposes.

1. Introduction

Photodynamic therapy is a promising cancer treatment which involves a combination of visible light and a photosensitizer. Each factor is harmless by itself, but after combination with oxygen they trigger a sequence of photochemical and photobiological processes damaging intracellular organelles and leading to cell death.[1] Compared to traditional cancer therapies such as surgery, radiation therapy or chemotherapy, PDT offers the opportunity to destroy tumors cells effectively and selectively, without damaging surrounding healthy tissue.[1,2] However, search for novel, better photosensitizers continues as the majority of current photosensitizers do not exhibit desirable combinations of chemical, photophysical and biological properties, crucial for improved efficacy of PDT against various types of cancer. The main features of an efficient photosensitizer include: (1) preferential uptake and/or retention by tumor tissues, (2) rapid clearance from surrounding normal tissue, that is, low systemic toxicity, (3) low dark toxicity, (4) high quantum yield of singlet oxygen formation ($^1O_2$), (5) high extinction coefficient in the 600–900 nm range where tissue penetration of light is maximum, (6) high chemical purity and well-known composition, (7) low aggregation tendency and (8) chemical properties conducive for efficient drug administration.[3,4] Recent synthetic activity has led to a great number of potential photosensitizers and among them chlorins are the most promising candidates.[5] Chemically, chlorins have a porphyrin skeleton-based core with a double bond in one of the four pyrrole rings reduced (Fig. 1).[6]

This structural modification strengthens the longest-wavelength absorption band and moves the λ_{max} further to the red end of the

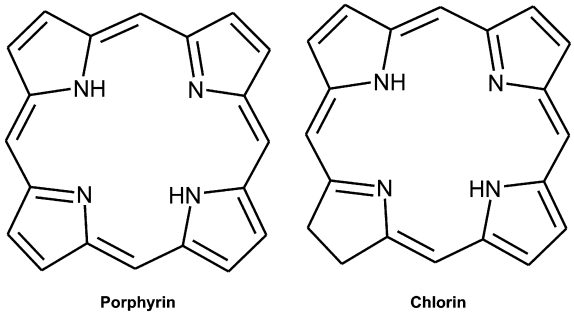

Figure 1. Parent structures of chlorin and porphyrin photosensitizers.

* Corresponding author. Tel.: +48 32 359 21 40; fax: +48 32 258 84 31.
E-mail addresses: agnieszka.szurko@us.edu.pl (A. Szurko), mont@chemie.uni-bremen.de (F.-P. Montforts).

0968-0896/$ - see front matter © 2009 Elsevier Ltd. All rights reserved.
doi:10.1016/j.bmc.2009.10.029

spectrum (Fig. 2).[5,7] In chlorin-type photosensitizers the red-shifted absorption band (λ_{max} = 660 nm, ε = 41,000 $mol^{-1}\,dm^3\,cm^{-1}$) allows for deeper light penetration into tissue than in the case of porphyrin-type compounds (λ_{max} = 626 nm, ε = 4400 $mol^{-1}\,dm^3\,cm^{-1}$). The excitation coefficient of chlorins is about ten times higher than that of the corresponding porphyrins.[8] Furthermore, they seem to be highly efficient singlet oxygen generators.[9] Such photophysical properties fulfill the requirements for a good photosensitizer and make chlorins promising candidates for applications in PDT.

This study investigated selected physical, chemical and biological properties of a new chlorin-type photosensitizer. We present vibrational spectra of the examined compound and the results of biological studies. Initial in vitro experiments explored several experimental parameters such as photosensitizer concentration, time of transfection or compound delivery method into the cells. Besides cytotoxicity and phototoxicity in vitro examinations included subcellular localization studies. Possible damaging effects of the studied chlorin on DNA and cytoskeleton were studied using immunocytochemical staining of actin microfilaments followed by fluorescence microscopy.

2. Results and discussion

2.1. Chemistry lab

The novel chlorin dicarboxylic acid **4** was prepared from the red blood pigment heme in a multistep synthetic sequence (Scheme 1), which was formerly developed for the construction of lipophilic chlorins.[8,10–13] The synthetic sequence started with copper(II)deuteroporphyrin dimethylester **1** a direct degradation product of the easily accessible red blood pigment heme. The copper(II)deuteroporphyrin dimethylester **1** was transformed into its 3-heptanoyl substituted derivative **2** by Friedel–Crafts-acylation. Copper removal and sodium borohydride reduction yielded the hydroxyheptyl porphyrin **3**. Porphyrin **3** was then reacted to the target chlorin **4** by Claisen rearrangement, hydrogenation and hydrolysis of the propionic acid esters. The hydrogenation procedure formed a 3:2 mixture of *cis*/*trans* stereoisomers, which could be separated by HPLC [LiChrosorb RP18 (Merck), methanol, 1 ml/min, *cis* isomer: t_R = 8.2 min; *trans* isomer: t_R = 7.3 min] for analytical purposes. Samples of the pure stereoisomers were hydrolyzed separately to yield *cis* and *trans* chlorin dicarboxylic acid **4** which were structurally characterized. For biological studies a mixture of *cis*/*trans* isomers were used because a chromatographic separation on a preparative scale seemed too tedious. By reversed phase HPLC it was demonstrated that the lipophilicity of the *cis*/*trans* isomers of both heptyl chlorin dicarboxylic acids is very close together and in a similar range as that of the active components of the widely used PDT photosensitizer Photofrin II.[8] We are conscious of well-known fact that constitutional isomers usually have similar photophysics and photochemistry characteristic, but sometimes different biological properties. Their different configurations may be induced more or less selectively in organism localization and uptake by certain cells.[14] Kasugai et al. compared the effect on cell death of water-soluble *cis*- and *trans*-Fe–porphyrins using the different cell lines (Walker 256 and H-4-II-E as cancer cells and FR and BRL-3A as normal cells). They clarified that *cis*-Fe–porphyrin showed a good cytotoxicity to cancer cells, while for *trans*-isomer no cytotoxic effects were observed. Furthermore, they demonstrated that the amount of *cis*-isomer inside the cell was enhanced compared with *trans*-isomer and only *cis*-isomer caused DNA damage in a cell.[15] Obviously, we realize that it was different case, also due to classification of compounds to metalloporphyrins. We strongly believe that in our *cis*/*trans* isomers changes in distribution of electrons are minimal, therefore usage of mixture of isomers shouldn't affect biological activity.

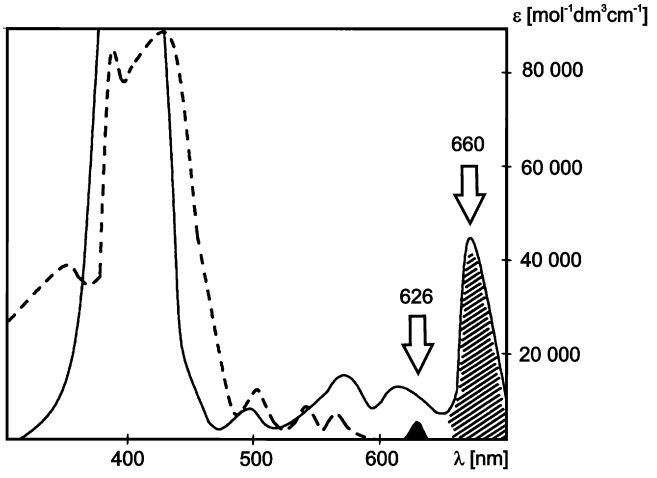

Figure 2. UV–vis absorption spectrum of chlorin (solid line) and porphyrin (broken line).

2.2. Physical studies

2.2.1. Interpretation of vibrational IR spectrum of chlorin 4

Infrared (IR) spectroscopy is a useful technique for characterizing materials and providing information about their structure and dynamics. In the present study vibrational spectroscopy was used to confirm the molecular structure of the studied chlorin derivative **4**. The strongest IR bands and their assignments are listed in Table 1. The assignment was done on the base of density functional theory (DFT) calculation. The geometry of the molecule was optimized and harmonic frequencies were calculated using B3LYP/6-31G(d,p) model. The calculated force fields were scaled using the scaled quantum mechanical force field method (SQM), giving better to fit to experimentally observed vibrational fundamentals and infrared intensities.[16] All calculations were performed using PQS ab initio program package. The assignment was also compared with those reported by Berezin et al.[17,18] Obtained experimental and calculated IR spectra of chlorin **4** are shown in Figure 3.

2.3. Biological studies

2.3.1. Dark toxicity and PDT effects of the studied chlorin in LLC cells

The experiments were performed to determine the degree of dark toxicity and PDT efficiency of chlorin derivative **4** on LLC cells. Cell proliferation was evaluated by measuring cell metabolic activity using MTS assay. In these studies cells were transfected with the examined compound for 4 or 12 h, as described in Section 5.3.3. The viability assay was carried out 24 h post-irradiation. The experimental results are shown in Figure 4. It can be seen that light or photosensitizer separately did not lead to any significant decrease of survival fraction. For the examined concentrations no negative cytotoxic effects of the studied compound were observed. After irradiation in the absence of the compound, decreased cell viability was not noticed. Cells death was only triggered by a combination of the photosensitizer and light. Following PDT, cell survival fraction decreased when the concentration of chlorin was raised. The therapeutic effect was observed at 0.5 μM chlorin concentration and up.

These results were compared to those of experiments involving Photofrin® (PH). The comparison is shown in Figure 5. For the examined concentrations of Photofrin® no considerable therapeu-

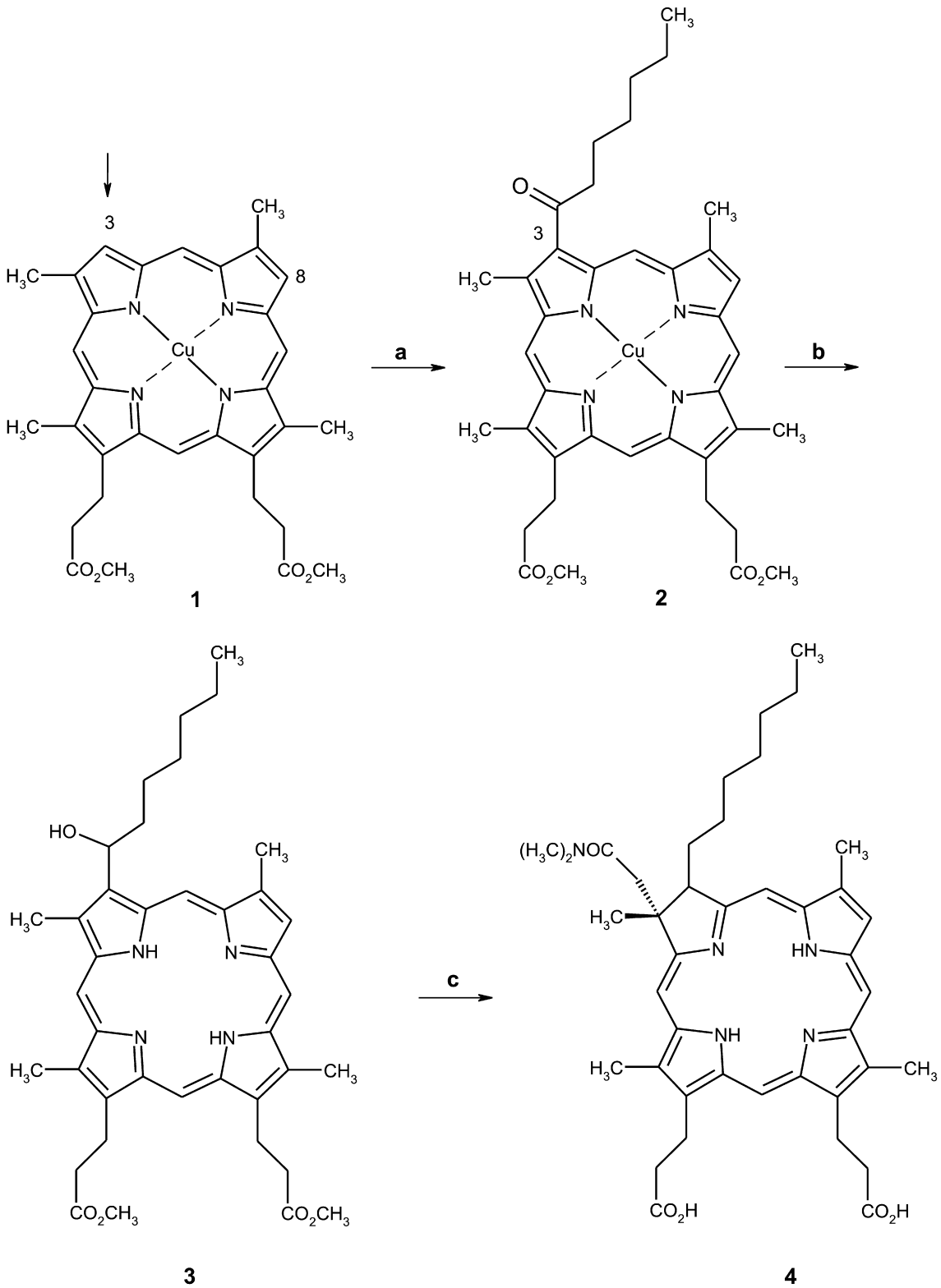

Scheme 1. Synthesis and structure of the studied chlorin photosensitizer (CHL) **4**. Reaction conditions: (a) (n-$C_6H_{13}CO)_2O$, $SnCl_4$, CH_2Cl_2, −15 °C, 93% mixture of 3,8 constitutional isomers; (b) (1) mixture of constitutional isomers, concd H_2SO_4, (2) CH_2N_2, ether, 95% for (1) (2), (3) mixture of constitutional isomers, $NaBH_4$, CH_2Cl_2, MeOH, −20 °C, 83% mixture, (4) prep. MPLC: SiO_2 (Matrex), CH_2Cl_2/EtOAc (6:1), 37% 3-isomer, 25% 8-isomer, 20% 3,8-mixture; (c) (1) $CH_3C(OCH_3)_2$ $N(CH_3)_2$, o-xylene, 160 °C, 85%, (2) $Pd(OAc)_2$, $(EtO)_3SiH$, THF, rt, 85% 3:2 mixture of *cis*/*trans*-isomers, (3) KOH, H_2O, THF, 50 °C, 90% mixture of *cis*/*trans*-isomers.

tic effects were observed. Following PDT with 5 μM of PH the survival fraction (SF) was 60.7% (data not shown) whereas for the studied chlorin **4** a 10-fold lower concentration (0.5 μM) yielded a survival of only 22.3% of the cells.

2.3.2. Efficiency of liposomal chlorin delivery into LLC cells

PDT efficiency of the examined chlorin derivative **4** delivered into LLC cells via liposomal vehicles or after dissolving it in DMSO (dimethyl sulfoxide) was compared (Fig. 6). It can be seen that cell

Table 1
Interpretation of vibrational IR spectrum of chlorin **4**

Experimental frequencies (cm^{-1})	Group	Assignment
3342	N–H	N–H stretching vibrations in the pyrrole ring
2956, 2870	CH_3	CH_3 stretching
2925, 2854	CH_2	CH_2 stretching
1725, 1705	C=O	C=O stretching
1613, 1559,1544, 1523		Chlorin stretching in-plane vibrations
1503, 1456	CH_2	CH_2 bending (scissoring)
1397,1380	CH_2	CH_2 bending (wagging)
1352		Chlorin stretching in-plane vibrations
1260	C(=O)–C	C(=O)–C stretching
1234	N–C(H_3)	N–C(H_3) stretching
1203	C–H	Chlorin out-of-plane vibrations
1150	C(=O)–N	C(=O)–N stretching
1105	C–C	Chlorin out-of-plane vibrations
970		Chlorin stretching in-plane vibrations
919	C–C	C–C stretching vibrations in alkyl chain
853,830		Chlorin out-of-plane deformation
718	CH_2	CH_2 twisting vibrations in $-C_7H_{15}$
704		Chlorin in-plane deformation
671	C–C(H_3)	C–C(H_3) stretching
620		Chlorin out-of-plane deformation

survival fraction for photosensitizer dissolved in DMSO was significantly higher than that when liposomal delivery was used. Using DMSO-dissolved chlorin the survival fraction was 70.6% (for 4-h transfection) and 74.4% (for 12-h transfection) whereas in experiments performed under similar conditions, but with liposomal vehicles, the survival fractions were 20.3% and 34.8%, respectively. Confocal microscopy showed that the examined compound was efficiently delivered into LLC cells via liposomal vehicles. This finding is of considerable significance for PDT treatment with the studied chlorin species **4**.

2.3.3. Confocal microscopy studies of intercellular distribution of the chlorin photosensitizer 4

Intracellular localization of photosensitizers plays a crucial role for the outcome of PDT treatment as it determines the site of primary photodamages and the type of cellular response to the therapy. Confocal laser scanning microscopy was used to identify the site of photosensitizer accumulation inside LLC cells. As a marker, a fluorescent dye CMFDA was employed. Argon ion laser (488 nm) and helium neon laser (543 nm) served as light sources to excite CMFDA and the studied compound **4**, respectively. After excitation the chlorin photosensitizer **4** emits bright-red fluorescence whereas that of CMFDA is bright green. Figure 7 shows that the examined compound **4** delivered via liposomal emulsion was efficiently transferred into LLC cells. After entry into cells the photosensitizer was localized in the cytoplasm around the nucleus of LLC cells. In no case did the photosensitizer accumulate inside cell nucleus. The degree of the photosensitizer accumulation in LLC cells depended on transfection time (2–12 h) with intracellular retention getting stronger with increased transfection time. After 2 h only few cells incorporated the compound, whereas after 12 h all of the examined cells showed intense bright-red fluorescence originating from the internalized compound.

2.3.4. Changes in F-actin and DNA structure following PDT

To investigate the PDT effects of the studied chlorin derivative **4** on cytoskeleton and DNA structures, cells were stained with FITC–phalloidin (λ_{ex} = 495 nm, λ_{em} = 513 nm) and DAPI (λ_{ex} = 358 nm, λ_{em} = 461 nm) to visualize F-actin and DNA. Analysis was carried out using fluorescence microscopy. The distribution of the markers in control cells is shown in Figure 8 A. In the control group (no photosensitizer, no irradiation) a network of F-actin filaments extending along the cell can be observed. Figure 8B shows the effects for cells incubated with the studied photosensitizer (2 μM) dissolved in DMSO, but without light irradiation. Some cells used for cytotoxicity assay were observed to have changed their morphology and become round. The fluorescence at the periphery of these cells

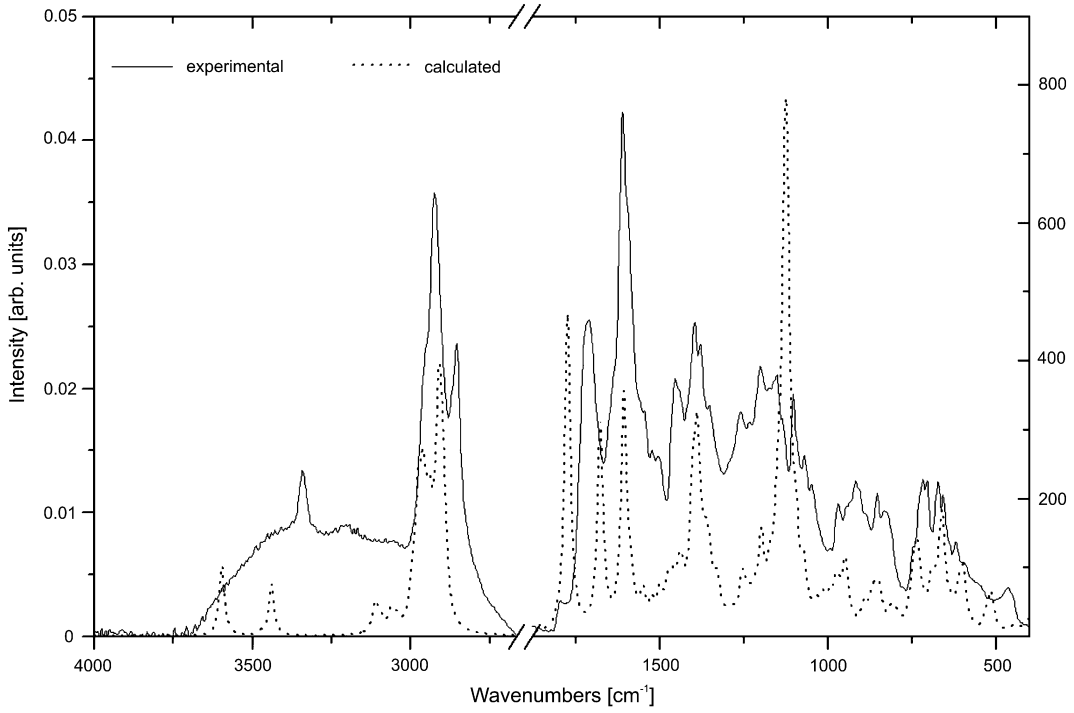

Figure 3. Experimental and calculated IR spectra of studied chlorin derivative **4**.

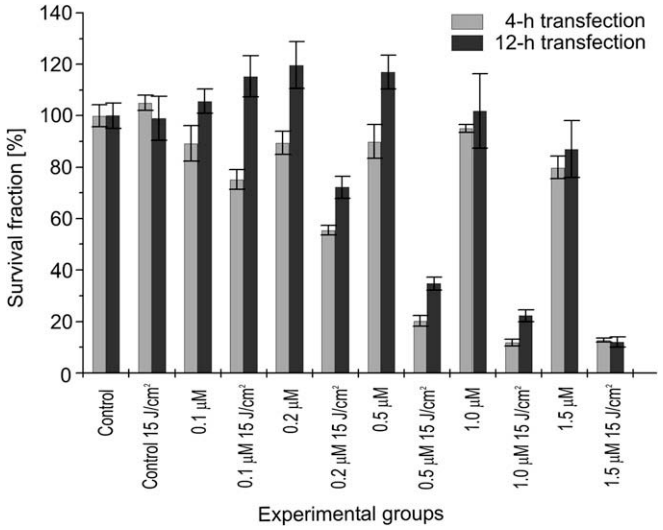

Figure 4. Dark toxicity and PDT efficiency. The studied chlorin **4** (0.1–1.5 μM) was delivered into LLC cells via liposomal vehicles. Following 4- or 12-h transfection and 24 h post-irradiation (15 J/cm^2) MTS assays were performed. Results are averaged from four independent experiments each performed in triplicate (for 4-h transfection) or six experiments performed in duplicate (for 12-h transfection).

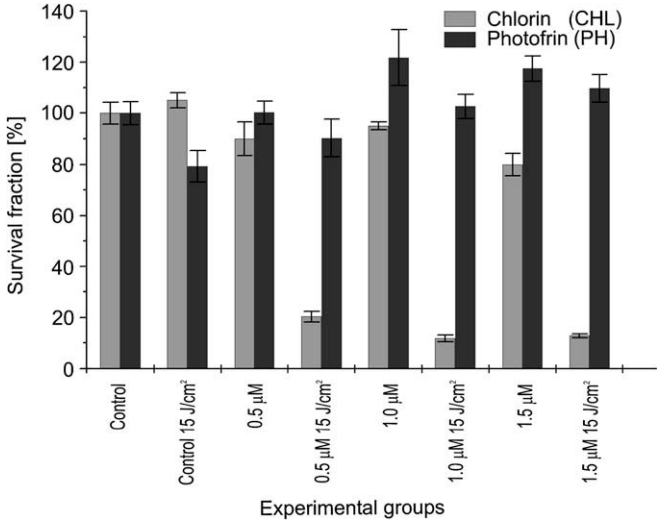

Figure 5. Comparison of dark toxicity and PDT efficiency of chlorin derivative **4** (CHL) (0.5 μM, 1.0 μM, 1.5 μM) and Photofrin® (PH) (0.5 μM, 1.0 μM, 1.5 μM). CHL was delivered into LLC cells via liposomal vehicles whereas PH solutions were prepared by diluting the stock solution with Opti-MEM (Gibco®) to desired final concentrations. Following 4-hour transfection and 24 h post-irradiation (15 J/cm^2) MTS assays were performed. Results are averaged from four (for CH) or three (for PH) independent experiments each performed in triplicate. All experiments were carried out under similar experimental conditions.

appeared to be stronger than in the center. These effects were stronger in groups treated with PDT (Fig. 8C). Following PDT with the chlorin photosensitizer we observed weaker fluorescence originating from the labeled filaments and uniform throughout cell volume. This indicates that after PDT the cytoskeleton of LLC cells looses F-actin construction. These modifications might be due to the condensation of F-actin. Following PDT, modifications in nucleus structure were also observed. In the control group nuclei had regular, oval form (Fig. 8B) whereas after PDT cell shape was more circular. Furthermore, in some cases DNA underwent intense defragmentation processes.

3. Discussion

Chlorin-type photosensitizers, due to their photophysical properties, are the topic of intensive research. Foscan® (*meta*-tetrahydroxyphenylchlorin, *m*-THPC) was approved by Food and Drug Administration (FDA) for clinical applications while others like NPe6 (mono-L-aspartyl chlorin e6) are in advanced stages of clinical trials.[19]

One of the most important photodynamic parameters in PDT is the quantum yield of singlet oxygen formation by a photosensitizer.[5] Montforts and co-workers synthesized and studied photophysical properties of a lipophilic *n*-heptyl chlorin derivative substituted at the dihydropyrrole ring (described as HCHL) with a structure very similar to the chlorin being the topic of current research. The photophysical parameters of the former compound, indicative of its photodynamic behavior, were excellent (λ_{max} = 645 nm, ε = 41,000 mol^{-1} dm^3 cm^{-1}, Φ_Δ = 0.6, Φ_T = 0.71, Φ_{fl} = 0.23).[20] The photophysical characterization of the novel compound yielded λ_{max} = 645 nm and ε = 33,700 mol^{-1} dm^3 cm^{-1} for *cis*-isomer and ε = 25,300 mol^{-1} dm^3 cm^{-1} for *trans*-isomer. The singlet oxygen quantum yield should be similar but it has not been studied yet.

Desirable biological properties like low dark toxicity and high photodynamic efficiency make the studied chlorin derivatives promising candidates for PDT applications. Preliminary research indicated that in the applied concentration range the studied compound did not induce cytotoxic effects in LLC cells and demonstrated photodynamic efficiency in LLC cell line. The damaging effects could be observed already after 40 min of transfection with the compound. Microscopic observation revealed that cells after irradiation were detached from the substratum and showed morphological changes such as shrinking and rounding up. The obtained results were compared with Photofrin®, the most widely used photosensitizer in clinical practice. The examined chlorin derivative was photodynamically efficient already at 0.5 μM concentration (SF = 20.3%) while with Photofrin®, at the same concentration and under analogical experimental conditions, no significant therapeutic effects were observed (SF = 90.4%). This indicates that the studied chlorin derivative offers the opportunity for being administered at relatively lower concentrations. In comparison, approximately 1–5 mg/kg of Photofrin® is needed for PDT, with the risk of long-term skin photosensitivity.[5] Due to stronger long-wavelength light absorption the second-generation photosensitizers can be used in smaller doses (0.2–0.5 mg/kg). A good example is provided by Foscan® use. This second-generation chlorine-type photosensitizer applied in head and neck tumor treatment is infused at very low doses,[21] typically ca. 0.1 mg/kg.[1,9,22]

In our in vitro experiments we have used liposomal carriers for efficient transport of the examined chlorin into cells. It has been known that liposomal delivery of photosensitizing agents can improve the selectivity of drug accumulation in cancer cells[23–26] and strongly increases photodynamic efficiency of the transported agents.[25,27] A liposomal formulation has been found to improve the tumor uptake of photosensitizer by the LDL-receptor-mediated endocytosis[5,27] because tumor cells are reported to express an elevated number of LDL-receptors due to their rapid proliferation and increased cholesterol demand for membrane synthesis.[9,27] A number of reports comparing the PDT outcome of liposomal versus non-liposomal photosensitizers provide strong evidence that, under identical conditions, liposomal formulations can be advantageous.[27] In 2007, Molinari et al. found total destruction of all cultures treated with cationic liposomes formed by DMPC (dimyristoyl-*sn*-*glycero*-phosphatidylcholine) and cationic gemini surfactant loaded with *m*-THPC in photodynamic therapy of glioma.[28] Pegaz et al. showed in pre-clinical in vivo investigations with *m*-THPC encapsulated in liposomal formulations that the formulation based on PEGylated liposomes technol-

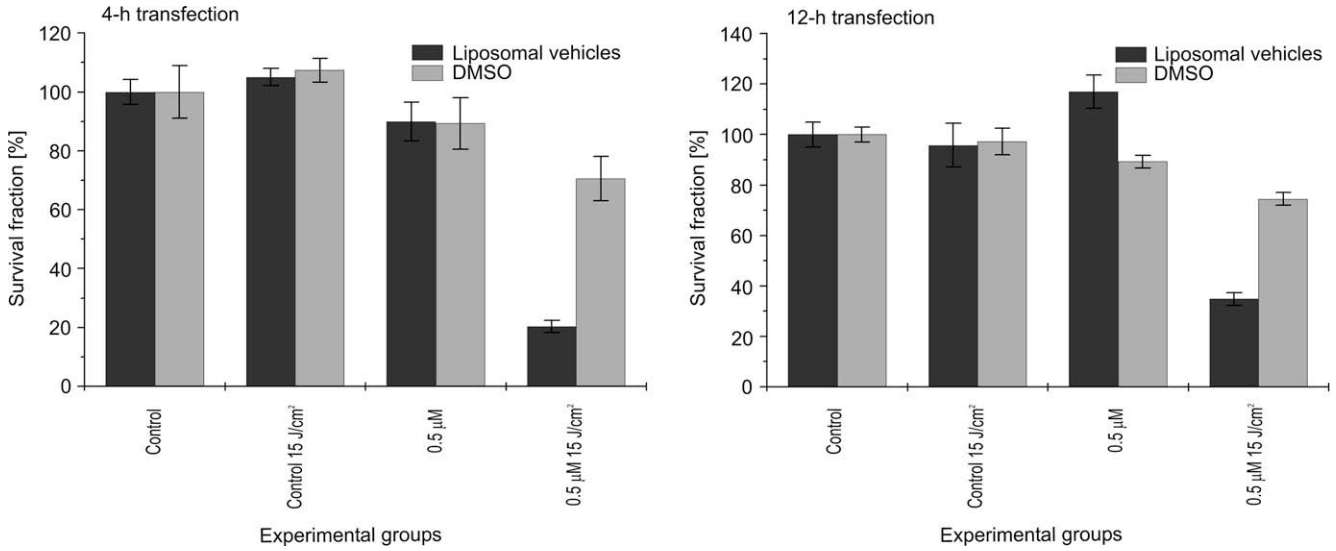

Figure 6. Dark toxicity and PDT efficiency of the studied chlorin **4** (0.5 μM) delivered into LLC cells via liposomal vehicles or via DMSO solution. Following a 4-h or 12-h transfection and 24 h post-irradiation (15 J/cm^2) cell proliferation was measured by MTS assay. Results are averaged from four independent experiments each performed in triplicate (for 4-h transfection) or six experiments performed in duplicate (for 12-h transfection) for liposomal transport and three experiments for DMSO. All experiments were carried out under similar experimental conditions.

ogy offers a suitable delivery system for PDT treatment of choroidal neovascularization associated with age-related macular degeneration.[29]

In the present study we compared the PDT efficiency of a novel chlorin derivative transferred into LLC cells via a liposomal vehicle or dissolved in DMSO. The latter turned out rather useless in our experiments. The survival fraction after 4 h of transfection was 70.6% while in experiments carried out under similar condition but using liposomally-entrapped chlorin a significantly stronger therapeutic effect (SF = 20.3%) was observed. Our findings show that liposomes can be a very efficient means of transferring the novel photosensitizer for PDT purposes. Postigo et al. have shown high photodynamic activity of chlorin-loaded liposomes in human skin fibroblast cells.[30] These researchers observed that after 1-h transfection DMSO-dissolved chlorins were more effective than liposome-delivered ones but for longer transfection times these differences vanished. Similar results were obtained by Wang in mice tissues[31] and by Rancan in Jukat cells.[32] Wang et al. have shown that the PDT efficiency of hypocrellin A dissolved in DMSO was highest when treatment was performed at 6 h post injection whereas for the compound transported via liposomes it was 12 h post injection, but in the case of liposomal transport the PDT efficiency expressed as tumor volume regression was much higher (87%) than that for DMSO (37%).[31]

The type of PDT response depends on intercellular localization of a photosensitizer.[33] After entry into cell photosensitizers accumulate preferentially in different subcellular compartments. For example, Photofrin® is taken up by the cell through passive diffusion or is brought into plasma membranes by phagocytosis whereas mono-*N*-aspartyl derivative of chlorin e6 is actively brought to the lysosomes by endocytosis.[34] The accumulation of the studied novel compound inside LLC cells was followed by confocal laser scanning microscopy. It was demonstrated that the examined compound was accumulated in the cytoplasm of LLC cells, especially in the perinuclear area. The degree of photosensitizer accumulation inside cells was proportional to drug concentration and increased with longer transfection times. As the studied photosensitizer did not accumulate in the nuclei of cells, the risk of its carcinogenic or mutation effect therefore seems small.

4. Conclusion

Cancers have widely different clinical patterns. Extending the use of PDT in clinical practice requires development of novel photosensitizers with optimized properties against different types of cancer. A novel lipophilic chlorin **4** was prepared from a readily accessible red blood pigment heme, according to a general synthetic route. The latter is valuable as it permits the construction of other chlorins with tailor-made properties. The photophysical properties combined with lipophilicity and biological functions of the novel chlorin **4** (like low dark toxicity and high photosensitivity) make it an attractive sensitizer for applications in photodynamic therapy (PDT). The chlorin synthesis opens the possibility for further structural modifications with regard to improved photophysical and biological activities. This potential provides an important motivation for continued investigation of the studied chlorin **4**.

5. Experimental section

5.1. 3,3′[*cis*, *trans*)-2-(Dimethylcarbamoyl-methyl)- 3-heptyl-2.7.12.18-tetramethyl-2.3-dihydro-21*H*.23*H*-chlorin-13.17-diyl]-dipropionic acid (4)

The analytical data confirmed the structure of the synthesized chlorin **4** which consists of a mixture of *cis*- and *trans*-isomers.

Selected physical data for the pure *cis*-isomer: Mp 106–109 °C. HPLC: LiChrosorb RP18; MeOH/H_2O (85:15); t_R = 5.5 min. HPLC: LiChrosorb RP18; MeOH/aqueous *n*-$Bu_4NH_2PO_4$ (2.5 mM/l, pH 2.5) (80:20); t_R = 64 min. IR (KBr): γ (cm^{-1}) = 3436 (s, OH, NH), 2910 (m, CH), 1720 (S, CO, acid), 1705 (s, CO, acid), 1605 (s, CO, amide). UV–vis ($CHCl_3$): λ_{max} (ε) = 393 nm (119,200), 490 (6600), 496 (6500), 525 (2300), 592 (2100), 645 (33,700). MS (FAB pos., TEG): *m*/*z* (%) = 696(100)[M+H$^+$]· 695(36)[M$^+$], 609(8) [M+H$^+$−C_4H_9NO]. Elemental Anal. Calcd for ($C_{41}H_{53}N_5O_5$, 695.90): C, 70.76; H, 7.68; N, 10.06. Found: C, 70.81; H, 7.70; N, 10.03. *trans*-Isomer: Mp 87–89 °C. HPLC: LiChrosorb RP18; MeOH/H_2O (85:15); t_R = 4.6 min. HPLC: LiChrosorb RP18; MeOH/aqueous *n*-$Bu_4NH_2PO_4$ (2.5 mM/l,

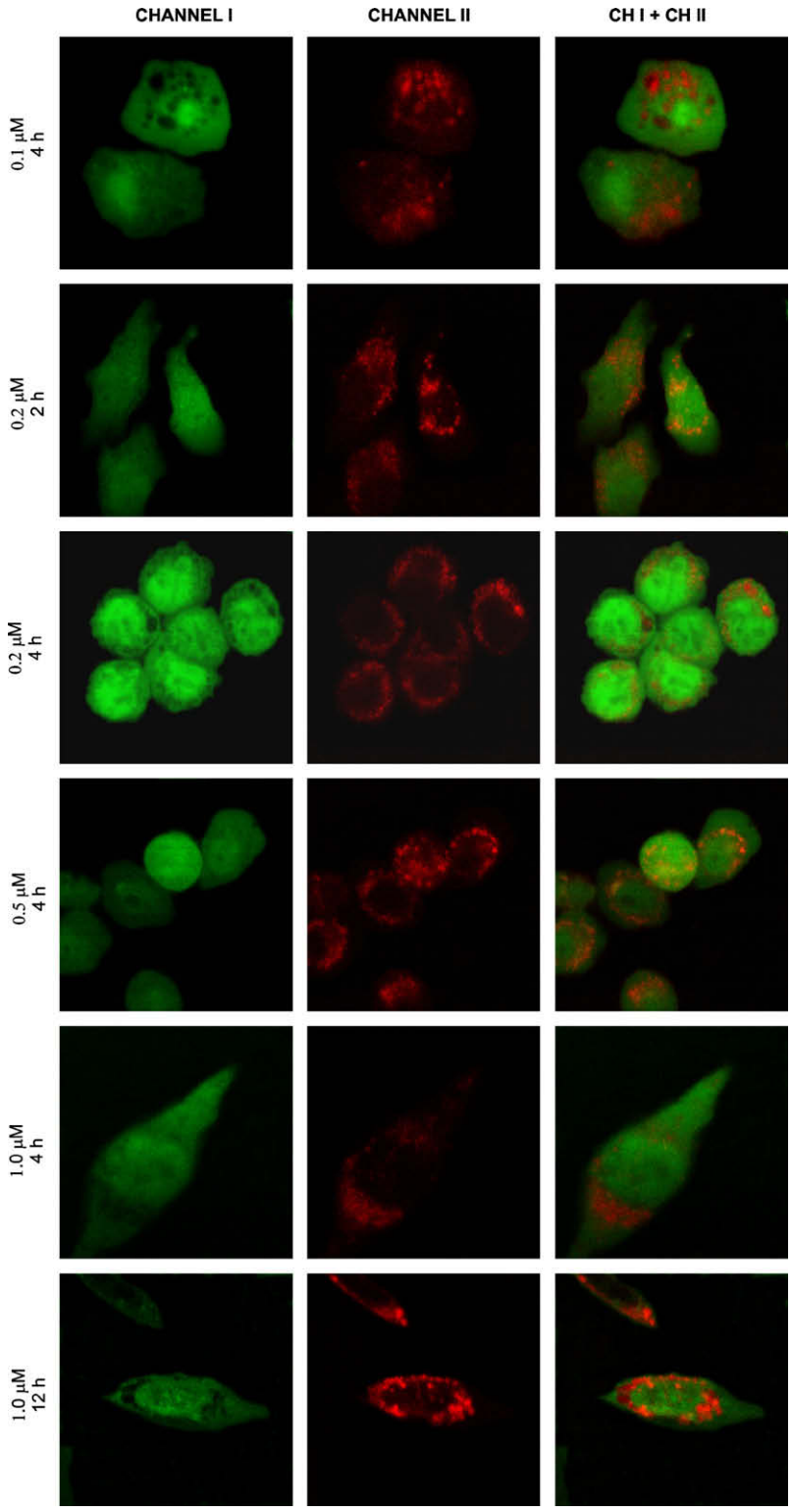

Figure 7. Intracellular distribution of the studied chlorin **4** in LLC cells performed by confocal microscopy. CMFDA (5-chloromethyl fluorescein diacetate) was used as a marker molecule. Helium neon laser (543 nm) and argon ion laser (488 nm) were used to excite CMFDA dye (channel I) and chlorin **4** (channel II), respectively.

pH 2.5) (80:20); t_R = 60 min. IR (KBr): γ (cm^{-1}) = 3310 (s, OH, NH), 2905 (m, CH), 1710 (s, CO, acids), 1600 (s, CO, amide). UV–vis ($CHCl_3$): λ_{max} (ε) = 393 nm (93,000), 490 (4900), 496 (4800), 525 (1600), 592 (1500), 645 (25,300). MS (FAB pos., TEG): *m*/*z* (%) = 696(100)[M+H$^+$], 695(27)[M$^+$], 609(72)[M+H$^+$−C_4H_9NO]. Elemental Anal. Calcd for ($C_{41}H_{53}N_5O_5$, 695.90): C, 70.76; H, 7.68; N, 10.06. Found: C, 70.63; H, 7.92; N, 9.76.

5.2. Physical studies

5.2.1. IR spectroscopy

Infrared (IR) spectrum was obtained using FTS 6000 spectrometer (Bio-Rad) connected with IR microscope UMA500. The spectral region was 500–4000 cm^{-1}. The measurement was performed on the sample in powder form.

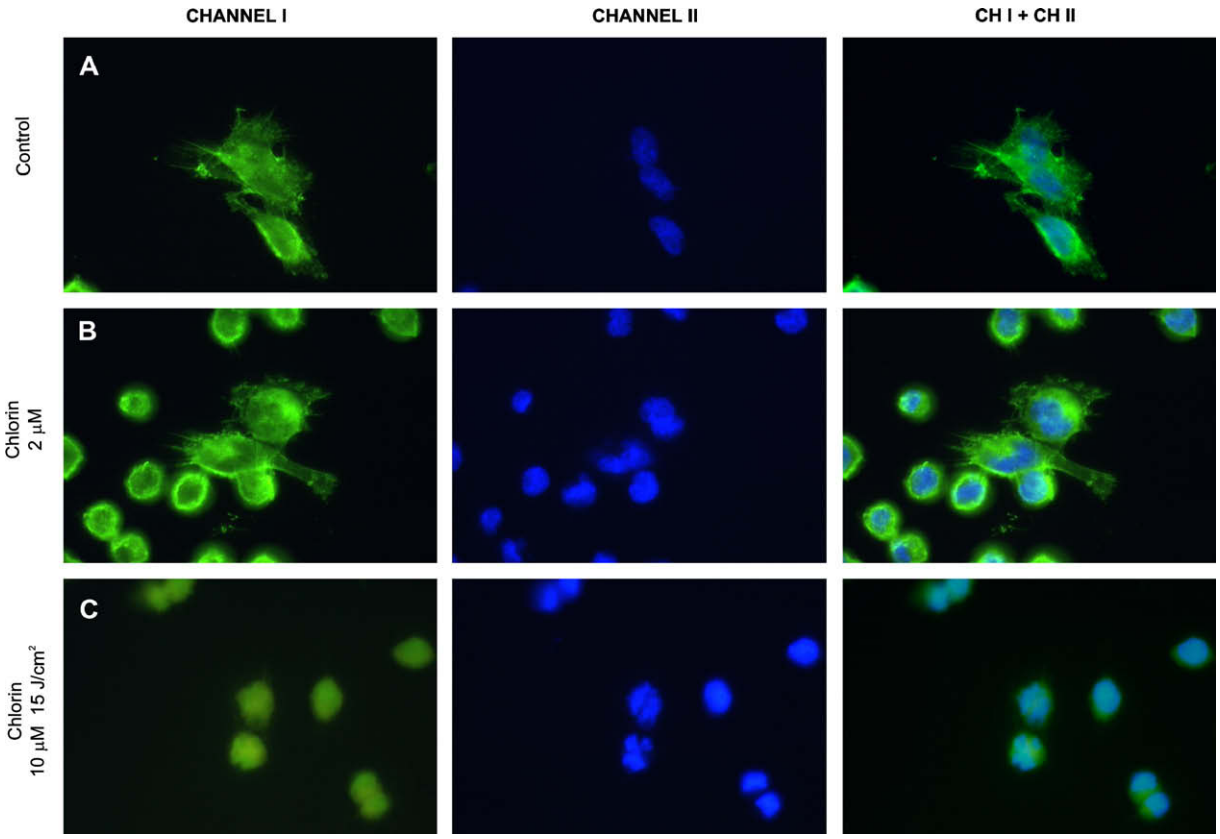

Figure 8. Changes in F-actin and DNA structure following PDT evaluated by fluorescence microscopy. LLC cells, after 4-h transfection with the studied chlorin dissolved in DMSO, were stained with FITC–phalloidin and DAPI to label F-actin (channel I) and DNA (channel II), respectively. Light dose for the irradiated group was 15 J/cm^2.

5.3. Biological studies

5.3.1. Cells and cell culture

Lewis lung carcinoma (LLC) cell line was propagated in 75 cm^2 flasks (Nunc) in humidified atmosphere with 5% CO_2 at 37 °C. Cells were maintained in Dulbecco's Modified Eagle's Medium (DMEM, Sigma) supplemented with 12% fetal bovine serum (FBS, Gibco®) and antibiotics (Gentamycin, Polfa).

5.3.2. Liposome preparation

Liposomes were prepared from synthetic phosphatidylcholine and cholesterol using the lipid film hydration method. The lipids were purchased from Avanti Polar Lipids (Birmingham, AL, USA). The lipids and the studied compound were dissolved at appropriate molar ratios in a mixture of chloroform and methanol (Sigma, 2:1 v/v). After solvent evaporation (rotary evaporator, 15 min/37 °C), the dry lipid film was hydrated (15 min/37 °C) and vortexed. Obtained multilayer vesicles were sonicated (Cole Parmer sonicator, medium power, 10 min). Liposome size was reduced by extrusion through polycarbonate filters (100 nm, pneumatic extruder device, Avestin). Obtained emulsions containing various concentrations of the studied photosensitizer were diluted with cell culture medium and used for biological experiments.

5.3.3. Cytotoxicity and PDT efficiency

LLC cells were seeded in 30-mm Petri dishes (Nunc) at a density of 3×10^5 cells/plates and incubated for 24 h under standard culture conditions. As controls, non-irradiated group without photosensitizer and groups incubated with various concentrations of photosensitizer but without light irradiation (dark control, cytotoxicity assay) were used. Other groups were subjected to photodynamic therapy or irradiation. After rinsing with phosphate buffered-saline (PBS, pH 7.2) the culture medium of one group was replaced by a medium with liposomes containing various concentrations of the photosensitizer to be studied and cells were incubated for 2–12 h. Appropriate solutions were prepared by diluting the emulsion of liposomes with different concentrations of the tested compound using Opti-MEM medium (Gibco®) for final concentrations (0.1–1.5 μM). Just before irradiation incubation medium was replaced with DMEM without phenol red. Cells were then irradiated from a distance of 3 cm with red light emitted by an halogen lamp (Optel) with 630 nm longpass filter. Total dosage of 15 J/cm^2 was calculated to be delivered to the cells during this treatment. A second irradiated group (not incubated with photosensitiser) was used to measure the effect of light only upon cell proliferation. Before irradiation, the medium was replaced with fresh culture medium and then cells were further incubated under standard culture conditions for 12 h or 24 h.

5.3.4. Proliferation assay

The number of viable cells was determined by MTS–tetrazolium reduction assay (Promega) and 3-cm plates. This colorimetric method is based on chemical reactions occurring in metabolically active cells when MTS reagent [3-(4,5-dimethylthiazol-2-yl)-5-(3-carboxymethoxyphenyl)-2-(4-sulfophenyl)-2*H*-tetrazolium] is reduced into a colored formazan. At the end of incubation, the medium was removed from culture and replaced with 700 μl DMEM without phenol red and 140 μl of MTS reagent. The quantity of soluble formazan, which is proportional to the number of viable cells, was estimated by measuring its spectrophotometric absorbance (490 nm) using a universal 96-well plate reader (Biotek Instruments). Background absorbance of a standard solution

(100 μl medium DMEM without phenol red, 20 μl MTS reagent) was subtracted. The surviving cell fraction was calculated as the percentage of viable cells relative to control samples (no photosensitizer, no irradiation).

5.3.5. Intracellular localization

Confocal laser scanning microscopy (using LSM 510 equipment, Carl Zeiss GmbH) was used to visualize subcellular localization of the photosensitizer. To visualize the shape of LLC cells and to verify accumulation of the studied photosensitizer the cultured cells were incubated with CellTracker Green CMFDA (Molecular Probes). This chloromethyl fluorescein derivative (5-chloromethyl fluorescein diacetate) can pass freely through cell membranes. The dye was excited using an argon ion laser (488 nm), whereas chlorin was excited using an helium neon laser (543 nm). Cells were seeded in four-well chambered coverglasses (Nunc) at a density of 4×10^4 cells/well and incubated under standard culture conditions. After 24 h of incubation cells were transfected (2–12 h) with media containing liposomal emulsions prepared with various concentrations of photosensitizer (0.1–1.0 μM). Cells were then washed in phosphate buffered-saline (PBS, pH 7.2) and placed in fresh culture medium. Thirty minutes before microscopic analysis cells were labeled with 5 μM CellTracker Green CMFDA.

5.3.6. Detection of cytoskeleton and DNA damages following PDT treatment

Fluorescein isothiocyanate (FITC) and phalloidin conjugate (Sigma, CAUTION: phalloidin is toxic; use following manufacturer's instructions) were used to label F-actin and to detect changes in cytoskeleton organization. Nuclear damage was detected with a fluorescent dye, 4′,6-diamidino-2-phenylindole (DAPI, Sigma). Cells were seeded in four-well chambered coverglasses (Lab-Tek II, Nunc) at a density of 1.5×10^4 cells/well and incubated 24 h under standard culture conditions. The culture medium was then replaced with medium including DMSO-dissolved photosensitizer. Drug solutions were prepared by diluting the chlorin stock (5 mg/ml DMSO) with Opti-MEM (Gibco®) to desired final concentrations (2–15 μM). The highest DMSO concentration did not exceed 0.3%. After 4-h transfection the irradiated and non-irradiated groups were treated as described in Section 5.2.3. Subsequent to incubation (18 h) the cells were placed in fresh culture medium and incubated for another 2 h. Medium was then removed and cells were washed (5 min) with phosphate buffered-saline (PBS, pH 7.2). The cells were then fixed with 4% paraformaldehyde (PFA) for 10 min and washed again with PBS (5 min). Subsequent to fixing, cells were permeabilized with 0.1% Triton X-100 and washed again with PBS (3×5 min). The samples were incubated in the dark with FITC–phalloidin (1:100) for one hour at room temperature. Furthermore, to visualize nuclei the cells also were incubated with DAPI (1:500, 15 min) which passes easily through cell membrane and binds strongly to DNA. Samples were mounted under glass coverslides using a drop of fluorescent mounting medium (DACO) and observed under a fluorescent microscope (Axiovert 135, Carl Zeiss).

Acknowledgments

This work was supported in part by the Polish Ministry of Science and Higher Education (Grant No. 0538/R/T02/2007/03).

We gratefully acknowledge Alexei Mikhailov contribution to immunocytochemical investigation.

References and notes

1. Sharman, W. M.; Allen, C. M.; Lier, J. E. *Drug Discovery Today* **1999**, *4*, 507.
2. Konan, Y. N.; Gurny, R.; Allémann, E. *J. Photochem. Photobiol., B* **2002**, *66*, 89.
3. You, Y.; Gibson, S. L.; Detty, M. R. *J. Photochem. Photobiol., B* **2006**, *85*, 155.
4. Král, V.; Králová, J.; Kaplánek, R.; Bříza, T.; Martásek, P. *Physiol. Res.* **2006**, *55*, S3.
5. Nyman, E. S.; Hynninen, P. H. *J. Photochem. Photobiol., B* **2004**, *73*, 1.
6. DeRosa, M. C.; Crutchley, R. J. *Coord. Chem. Rev.* **2002**, *233–234*, 351.
7. Castano, A. P.; Demidova, T. N.; Hamblin, M. R. *Photodiag. Photodyn. Ther.* **2004**, *1*, 279.
8. Montforts, F.-P.; Gerlach, B.; Haake, G.; Höper, F.; Kusch, D.; Meier, A.; Scheurich, G.; Brauer, H.-D.; Schiwon, K.; Schermann, G. *Proc. SPIE* **1994**, *2325*, 29.
9. MacDonald, I. J.; Dougherty, T. J. *J. Porphyrins Phthalocyanines* **2001**, *5*, 105.
10. Montforts, F.-P.; Meier, A.; Haake, G.; Höper, F. *Tetrahedron Lett.* **1991**, *32*, 3481.
11. Haake, G.; Hoeper, F.; Meier, A.; Montforts, F.-P.; Scheurich, G.; Zimmermann, G. *Liebigs Ann. Chem.* **1992**, 325.
12. Kusch, D.; Meier, A.; Montforts, F.-P. *Liebigs Ann. Chem.* **1995**, 1027.
13. Montforts, F.-P.; Kusch, D.; Höper, F.; Braun, S.; Gerlach, B.; Brauer, H.-D.; Schermann, G.; Moser, J. G. *Proc. SPIE* **1996**, *2675*, 212.
14. Wang, J.; Liu, H.; Xue, J.; Jiang, Z.; Chen, N.; Huang, J. *Chin. Sci. Bull.* **2008**, *53*, 1657.
15. Kasugai, N.; Murase, T.; Ohse, T.; Nagaoka, S.; Kawakami, H.; Kubota, S. *J. Inorg. Biochem.* **2002**, *91*, 349.
16. Baker, J.; Jarzecki, A. A.; Pulay, P. *J. Phys. Chem.* **1998**, *102*, 1412.
17. Berezin, K. V.; Nechaev, V. V. *Chem. Nat. Compd.* **2003**, *39*, 540.
18. Berezin, K. V.; Nechaev, V. V. *J. Appl. Spectrosc.* **2004**, *71*, 307.
19. Huang, Z. *Technol. Cancer Res. Treat.* **2005**, *4*, 283.
20. Grewer, C.; Schermann, G.; Schmidt, R.; Völcker, A.; Brauer, H.-D.; Meier, A.; Montforts, F.-P. *J. Photochem. Photobiol., B* **1991**, *11*, 285.
21. Allison, R. R.; Cuenca, R. E.; Downie, G. H.; Camnitz, P.; Brodish, B.; Sibata, C. H. *Photodiag. Photodyn. Ther.* **2005**, *2*, 205.
22. Dougherty, T. J.; Gomer, C. J.; Henderson, B. W.; Jori, G.; Kessel, D.; Korbelik, M.; Moan, J.; Peng, Q. *J. Natl. Cancer Inst.* **1998**, *90*, 889.
23. Chen, B.; Pogue, B. W.; Hasan, T. *Exp. Opin. Drug Delivery* **2005**, *2*, 477.
24. Reddi, E. *J. Photochem. Photobiol., B* **1997**, *37*, 189.
25. Hoebeke, M. *J. Photochem. Photobiol., B* **1995**, *28*, 189.
26. Osterloh, J.; Vicente, M. G. H. *J. Porphyrins Phthalocyanines* **2002**, *6*, 305.
27. Derycke, A. S. L.; de Witte, P. A. M. *Adv. Drug Delivery Rev.* **2004**, *56*, 17.
28. Molinari, A.; Colone, M.; Calcabrini, A.; Stringaro, A.; Toccacieli, L.; Arancia, G.; Mannino, S.; Mangiola, A.; Maira, G.; Bombelli, C.; Mancini, G. *Toxicol. In Vitro* **2007**, *21*, 230.
29. Pegaz, B.; Debefve, E.; Ballini, J.-P.; Wagniéres, G.; Spaniol, S.; Albrecht, V.; Scheglmann, D. V.; Nifantiev, N. E.; Bergh, H.; Konan-Kouakou, Y. N. *Eur. J. Pharm. Sci.* **2006**, *28*, 134.
30. Postigo, F.; Sagristá, M. L.; De Madariaga, M. A.; Nonell, S.; Mora, M. *Biochim. Biophys. Acta* **2006**, *1758*, 583.
31. Wang, Z.-J.; He, Y.-Y.; Huang, C.-G.; Huang, J.-S.; Huang, Y.-C.; An, J.-Y.; Gu, Y.; Jiang, L.-J. *Photochem. Photobiol.* **1999**, *70*, 773.
32. Rancan, F.; Wiehe, A.; Nöbel, M.; Senge, M. O.; Al Omari, S.; Böhm, F.; John, M.; Röder, B. *J. Photochem. Photobiol., B* **2005**, *78*, 17.
33. Almeida, R. D.; Manadas, B. J.; Carvalho, A. P.; Duarte, C. B. *Biochim. Biophys. Acta* **2004**, *1704*, 59.
34. Allison, R. R.; Mota, H. C.; Bagnato, V. S.; Sibata, C. H. *Photodiagnosis Photodyn. Ther.* **2008**, *5*, 19.